

## Strange quark mass effect in $B_s \rightarrow \gamma\gamma, \gamma\ell\bar{\ell}$ decays

Dong-Hao Li<sup>1,2,‡</sup>, Lei-Yi Li<sup>1,2,†</sup>, Cai-Dian Lü<sup>1,2,§</sup> and Yue-Long Shen<sup>3,\*</sup>

<sup>1</sup>*Institute of High Energy Physics, CAS, P.O. Box 918(4), Beijing 100049, China*

<sup>2</sup>*School of Physics, University of Chinese Academy of Sciences, Beijing 100049, China*

<sup>3</sup>*College of Physics and Photoelectric Engineering, Ocean University of China, Qingdao 266100, China*



(Received 15 May 2022; accepted 31 October 2022; published 29 November 2022)

In this paper we investigate the next-to-leading power contribution to the  $B_s \rightarrow \gamma\gamma$  and  $B_s \rightarrow \gamma\ell\bar{\ell}$  decays from the strange quark mass effect with the dispersion approach which is QCD inspired and more predictive. We present the analytic expression of the quark mass contribution in the  $B_s \rightarrow \gamma\gamma$  and  $B_s \rightarrow \gamma\ell\bar{\ell}$  decays, together with a new term that is missed in the previous study. We also evaluate the resolved photon contribution from the A-type amplitude in  $B_s \rightarrow \gamma\ell\bar{\ell}$  decay. The numerical results of the strange quark mass contribution to the  $B_s \rightarrow \gamma\gamma$  decay is about 6% relative to the total branching ratio, while it is relatively small in the  $B_s \rightarrow \gamma\ell\bar{\ell}$  decay due to the large resonance contribution.

DOI: 10.1103/PhysRevD.106.094038

### I. INTRODUCTION

The double radiative decay  $B_s \rightarrow \gamma\gamma$  and radiative leptonic decay  $B_s \rightarrow \gamma\ell\bar{\ell}$  are of great importance to the determination of the parameters of the light cone distribution amplitudes (LCDA) of  $B_s$  meson, which is the fundamental nonperturbative input in the study on the  $B_s$  meson decays. They are also sensitive to the new physics effect since they are induced by the flavor-changing neutral-current processes [1,2], and the latter also serves as an important background of the leptonic decay  $B_s \rightarrow \ell^+\ell^-$ . Relatively little attention has been paid to these modes due to their small branching ratios, while the current machines with high luminosity such as LHC and SuperKEKB have the capability to detect these decays [3]. The experimental progresses on these decay modes raise the necessity of more precisely theoretical predictions, which have been improved in several aspects.

A comprehensive study on the  $B_{d,s} \rightarrow \gamma\gamma$  decays is presented in [4], where both leading-power contributions and power-suppressed contributions to the decay amplitude have been analyzed in detail. The leading power amplitude of  $B_{d,s} \rightarrow \gamma\gamma$  can be factorized into the convolution of the effective Wilson coefficients, the jet function and the

leading-twist LCDA of  $B_{d,s}$  meson [5], where both the effective Wilson coefficients and the jet function have been provided up to two-loop order in QCD [6,7], and the next-to-leading logarithm resummation has been performed within the framework of soft-collinear effective theory [8,9]. Various subleading power contributions have also been investigated, including the power-suppressed local contribution, the power suppressed nonlocal contribution from the hard-collinear propagator, the power suppressed term in the heavy quark expansion, the contribution from high twist LCDAs of  $B$  meson, the strange quark mass effects and resolved photon contribution. Some power-suppressed contributions are proved to be factorizable, such as the nonlocal contributions from the hard-collinear propagator, from the heavy quark expansion, and from the high twist LCDAs, while the factorization theorem cannot be applied to the strange quark mass contribution due to the emergence of endpoint singularity.

As endpoint singularity appears in the convolution between the jet function and leading-twist LCDA of  $B_s$  meson in the contribution from the strange quark mass term in  $B_s \rightarrow \gamma\gamma$  decay, it is a tough task to predict this contribute with high credibility. A parametrization method is employed in [4], which is model dependent with sizable theoretical uncertainty. In this paper we will adopt an alternative method with better predictive power, which is called dispersion approach in the literature. This approach has been widely used in the evaluation of the power suppressed contribution in the exclusive processes such as  $\gamma^*\gamma \rightarrow \pi$ ,  $B \rightarrow \gamma\nu\ell$  *et al.* to estimate the contribution from the resolved photon effect [10–15], and the results are consistent with the prediction from employing the photon LCDAs [16–22]. The basic idea of the dispersion method is to take the photon momentum (from the QED vertex) off

\*Corresponding author.  
shenylmeteor@ouc.edu.cn

†lileiyi@ihep.ac.cn

‡lidonghao@ihep.ac.cn

§lucd@ihep.ac.cn

Published by the American Physical Society under the terms of the [Creative Commons Attribution 4.0 International license](https://creativecommons.org/licenses/by/4.0/). Further distribution of this work must maintain attribution to the author(s) and the published article's title, journal citation, and DOI. Funded by SCOAP<sup>3</sup>.

shell and replace the endpoint region of the convolution between the jet function and the LCDA of  $B_s$  meson with hadronic representation of the correlation functions below the effective continuum threshold, and take the  $q^2 = 0$  limit after the replacement. The power suppressed resolved photon contribution to the helicity form factors of  $B_s \rightarrow \gamma\gamma$  decay is obtained through the difference between the hadronic representation with isolated vector meson state and the endpoint region of the factorization formula of the correlation function at leading power [4]. After including the strange quark mass contribution to the correlation function, we can reach the contribution from the resolved photon and the strange quark mass, respectively.

The  $B_{d,s} \rightarrow \gamma\ell\bar{\ell}$  decays in the kinematic region of large photon energy was intensively analyzed with QCD factorization techniques recently [23], which constructs a systematic expansion in inverse powers of large photon energy and heavy quark mass. The leading-power contribution has been split into the A-type amplitude  $\bar{\mathcal{A}}_{A\text{-type}}$  (which accounts for the final-state photon emit from the constituents of  $B$  meson) and the B-type amplitude  $\bar{\mathcal{A}}_{B\text{-type}}$  (where the on shell photon is emitted directly from the dipole operators). The next-to-leading power (NLP) corrections to the amplitudes due to local and nonlocal A-type and B-type operators in the soft-collinear effective theory, as well as the local four-quark contributions, are also considered. The numerical calculation indicates that the NLP contribution can give rise to about 20%–30% correction to the branching ratios of the decay channels [23]. Compared with the large resonant amplitude, the strange quark mass effect can be safely neglected from the B-type amplitude. Both the resolved photon contribution and strange quark mass effect from the A-type amplitude have not been investigated in the  $B_s \rightarrow \gamma\ell\bar{\ell}$  decays, and we will fill this gap with a similar method as that in the  $B_s \rightarrow \gamma\gamma$  decay.

This article is organized as follows: In the next section we will review leading power and NLP contribution to the  $B_s \rightarrow \gamma\gamma$  and  $B_s \rightarrow \gamma\ell\bar{\ell}$  decays. In Sec. III we will take advantage of the dispersion approach to evaluate the NLP contribution from the quark mass term in the  $B_s \rightarrow \gamma\gamma$  and  $B_s \rightarrow \gamma\ell\bar{\ell}$  decays. The numerical result is given in Sec. IV. A summary is presented in the last section.

## II. THE AMPLITUDES OF $\bar{B}_s \rightarrow \gamma\gamma$ AND $\bar{B}_s \rightarrow \gamma\ell\bar{\ell}$ DECAYS

In order to express the decay amplitudes of the  $\bar{B}_s \rightarrow \gamma\gamma$  and  $\bar{B}_s \rightarrow \gamma\ell\bar{\ell}$  decays, we start with the effective weak Hamiltonian where the unitarity of the CKM matrix has been employed

$$\mathcal{H}_{\text{eff}} = \frac{4G_F}{\sqrt{2}} \sum_{p=u,c} V_{pb} V_{ps}^* \left[ \sum_{i=1}^2 C_i(\nu) P_i^{(p)}(\nu) + \sum_{i=3}^8 C_i(\nu) P_i(\nu) + \frac{\alpha_{\text{em}}}{4\pi} \sum_{i=9}^{10} C_i(\nu) P_i(\nu) \right] + \text{H.c.} \quad (1)$$

where the  $P_{1,2}^{(p)}$  are four-quark tree operators and the  $P_{3-6}$  are four quark QCD-penguin operators. The specific form of these operators and the corresponding Wilson coefficients  $C_i$  can be found in [4].  $P_7$  is the electromagnetic penguin operator which leads to  $b \rightarrow s\gamma$  transition at leading order in  $\alpha_s$ .  $P_8$  is the chromomagnetic penguin operator, and  $P_{9,10}$  are semileptonic operators for  $b \rightarrow q\ell\bar{\ell}$  transitions. These four effective operators are listed as

$$\begin{aligned} P_7 &= -\frac{g_{\text{em}} \bar{m}_b(\nu)}{16\pi^2} (\bar{s}_L \sigma^{\mu\nu} b_R) F_{\mu\nu}, \\ P_8 &= -\frac{g_s \bar{m}_b(\nu)}{16\pi^2} (\bar{s}_L \sigma^{\mu\nu} T^a b_R) G_{\mu\nu}^a, \\ P_9 &= -[\bar{s} \gamma^\mu P_L b][\bar{\ell} \gamma_\mu \ell], \\ P_{10} &= -[\bar{s} \gamma^\mu P_L b][\bar{\ell} \gamma_\mu \gamma_5 \ell], \\ P_L &= (1 - \gamma_5)/2, \end{aligned} \quad (2)$$

where  $\bar{m}_b(\nu)$  is the  $b$ -quark mass in the  $\overline{\text{MS}}$  scheme and the convention of the covariant derivative are the same with [4]. The amplitudes of  $\bar{B}_s \rightarrow \gamma\gamma$  and  $\bar{B}_s \rightarrow \gamma\ell\bar{\ell}$  decays can be written by the matrix elements of the effective Hamiltonian, i.e.,

$$\begin{aligned} \bar{\mathcal{A}}(\bar{B}_s \rightarrow \gamma\gamma) &= -\langle \gamma(k, \epsilon_1^*) \gamma(q, \epsilon_2^*) | \mathcal{H}_{\text{eff}} | \bar{B}_s(k+q) \rangle, \\ \bar{\mathcal{A}}(\bar{B}_s \rightarrow \gamma\ell\bar{\ell}) &= -\langle \gamma(k, \epsilon^*) \ell(p_\ell) \bar{\ell}(p_{\bar{\ell}}) | \mathcal{H}_{\text{eff}} | \\ &\quad \times \bar{B}_s(k+p_\ell+p_{\bar{\ell}}) \rangle. \end{aligned} \quad (3)$$

In the following, we quote the detailed expression of the decay amplitudes of  $\bar{B}_s \rightarrow \gamma\gamma$  and  $\bar{B}_s \rightarrow \gamma\ell\bar{\ell}$  processes which are obtained in [4,23] so that we can get the full amplitude after obtaining the contribution from the strange quark mass. For the  $\bar{B}_s \rightarrow \gamma\gamma$  decays, the amplitude including the power-suppressed contributions takes the form,

$$\begin{aligned} \bar{\mathcal{A}}(\bar{B}_s \rightarrow \gamma\gamma) &= -i \frac{G_F \alpha_{\text{em}}}{\sqrt{2}\pi} m_{B_s}^3 \epsilon_1^{*\mu}(p) \epsilon_2^{*\nu}(q) [(g_{\mu\nu}^\perp - i\epsilon_{\mu\nu}^\perp) \bar{\mathcal{A}}_L \\ &\quad - (g_{\mu\nu}^\perp + i\epsilon_{\mu\nu}^\perp) \bar{\mathcal{A}}_R], \end{aligned} \quad (4)$$

where  $\epsilon_1^{*\mu}$  and  $\epsilon_2^{*\nu}$  stand for the polarization vector of the two outgoing photons. The shorthand notations  $g_{\mu\nu}^\perp$  and  $\epsilon_{\mu\nu}^\perp$  are defined as

$$\begin{aligned} g_{\mu\nu}^\perp &\equiv g_{\mu\nu} - \frac{n_+^\mu n_{-\nu}}{2} - \frac{n_-^\mu n_{+\nu}}{2}, \\ \epsilon_{\mu\nu}^\perp &\equiv \frac{1}{2} \epsilon_{\mu\rho\tau} n_+^\rho n_-^\tau = \epsilon_{\mu\nu\rho\tau} n_+^\rho v^\tau, \end{aligned} \quad (5)$$

where the convention  $\epsilon_{0123} = -1$  has been adopted. The light cone vectors  $n_+, n_-$  have been introduced, which satisfy  $n_+^2 = 0$ ,  $n_-^2 = 0$  and  $n_+ \cdot n_- = 2$ . The amplitudes

$\bar{\mathcal{A}}_L$  and  $\bar{\mathcal{A}}_R$  are classified according to the polarization of the final state photons. The manifest expressions of  $\bar{\mathcal{A}}_L$  and  $\bar{\mathcal{A}}_R$  can be derived in the following

$$\begin{aligned}\bar{\mathcal{A}}_L &= \sum_{p=u,c} V_{pb} V_{ps}^* \sum_{i=1}^8 C_i \left[ F_{i,L}^{(p),\text{LP}} + F_{i,L}^{(p),\text{fac,NLP}} + F_{i,L}^{(p),\text{soft,NLP}} \right], \\ \bar{\mathcal{A}}_R &= \sum_{p=u,c} V_{pb} V_{ps}^* \sum_{i=1}^8 C_i \left[ F_{i,R}^{(p),\text{LP}} + F_{i,R}^{(p),\text{fac,NLP}} + F_{i,R}^{(p),\text{soft,NLP}} \right],\end{aligned}\quad (6)$$

where the three terms in the square bracket denote the leading power contribution, the factorizable NLP contribution and the power suppressed soft contribution, respectively. The factorizable NLP contribution collects various subleading power contributions, which is written as

$$\begin{aligned}\sum_{i=1}^8 C_i F_{i,L}^{(p),\text{fac,NLP}} &= C_7^{\text{eff}} \left[ F_{7,L}^{\text{hc,NLP}} + F_{7,L}^{m_q,\text{NLP}} + F_{7,L}^{A2,\text{NLP}} + F_{7,L}^{\text{HT,NLP}} + F_{7,L}^{e_b,\text{NLP}} \right] + \frac{f_{B_s}}{m_{B_s}} \left[ \mathcal{F}_V^{(p),\text{WA}} - \mathcal{F}_A^{(p),\text{WA}} \right], \\ \sum_{i=1}^8 C_i F_{i,R}^{(p),\text{fac,NLP}} &= \frac{f_{B_s}}{m_{B_s}} \left[ \mathcal{F}_V^{(p),\text{WA}} + \mathcal{F}_A^{(p),\text{WA}} \right].\end{aligned}\quad (7)$$

From the above equation we can see that only the contribution from weak annihilation mechanism, which is induced by the four-quark operators can give rise to the amplitude with right-handed polarized photon, since the other contributions induced by electromagnetic penguin operator are left handed in nature. All the amplitudes in (7) have been derived in [4]

with great detail. For  $\bar{B}_s \rightarrow \gamma\gamma$  decays, the nonvanishing strange quark mass leads to the term  $F_{7,L}^{m_s,\text{NLP}}$ , which will be specifically investigated in the next section.

For the  $\bar{B}_s \rightarrow \gamma\ell\bar{\ell}$  decays, the decay amplitude can be parametrized as

$$\bar{\mathcal{A}}(\bar{B}_s \rightarrow \gamma\ell\bar{\ell}) = ie \frac{\alpha_{\text{em}} G_F}{\sqrt{2}\pi} E_\gamma \epsilon_\mu^* [(g_\perp^{\mu\nu} - i\epsilon_\perp^{\mu\nu})(\bar{\mathcal{A}}_{LV}[\bar{u}\gamma_\nu v] + \bar{\mathcal{A}}_{LA}[\bar{u}\gamma_\nu\gamma_5 v]) - (g_\perp^{\mu\nu} + i\epsilon_\perp^{\mu\nu})(\bar{\mathcal{A}}_{RV}[\bar{u}\gamma_\nu v] + \bar{\mathcal{A}}_{RA}[\bar{u}\gamma_\nu\gamma_5 v])], \quad (8)$$

where  $V$  and  $A$  refer to the vector and axial-vector chirality structure of the lepton currents, respectively. The helicity amplitudes are given by

$$\begin{aligned}\bar{\mathcal{A}}_{hV} &= \sum_{p=u,c} V_{pb} V_{ps}^* \sum_{i=1}^9 C_i F_h^{(i)}, \\ \bar{\mathcal{A}}_{hA} &= \sum_{p=u,c} V_{pb} V_{ps}^* C_{10} F_h^{(10)}, \quad h = L, R,\end{aligned}\quad (9)$$

where the helicity form factors  $F_h^{(i)}$  contain both the leading power contribution and NLP contributions with the  $s\bar{s}$  resonance, which can be expressed by

$$F_h^{(i)} = F_h^{(i,\text{LP})} + F_h^{(i,\text{NLP})} + \mathcal{O}(\alpha_s^2, \alpha_s \lambda^2, \lambda^4), \quad (10)$$

where  $\lambda \equiv \Lambda_{\text{QCD}}/E_\gamma$  and the specific expression for these form factors have been given in [23]. In this paper the nonvanishing quark mass contributions are denoted by  $F_{m,h}^{(7A)}$ ,  $F_{m,h}^{(7B)}$ , and  $F_{m,h}^{(9,10)}$  in order to distinguish the contribution with the photon emission from  $P_7$  or  $P_{9,10}$ , and the

subscript  $h = L$  or  $R$  according to the helicity. In addition, we use  $F_{\text{soft},h}^{(7A)}$  and  $F_{\text{soft},h}^{(9,10)}$  to denote the contribution from the resolved photon.

### III. THE CONTRIBUTION FROM THE QUARK MASS TERM WITH DISPERSION APPROACH

Before constructing the theoretical framework to evaluate the contribution from the quark mass term, we show explicitly the mass term in the hard-collinear quark propagator (see Fig. 1) as

$$\begin{aligned}& \frac{\not{k} - \not{l} + m_s}{(k-l)^2 - m_s^2 + i0} \\ &= \frac{\not{k}}{n_+ k n_- (k-l) + i0} + \frac{-\not{l}}{n_+ k n_- (k-l) + i0} \\ &+ \frac{m_s}{n_+ k n_- (k-l) + i0} + \mathcal{O}\left(\frac{\Lambda_{\text{QCD}}^2}{m_b^2}\right),\end{aligned}\quad (11)$$

where  $l$  and  $k$  denote the momentum of the light strange quark inside the  $\bar{B}_s$  meson and the momentum of the

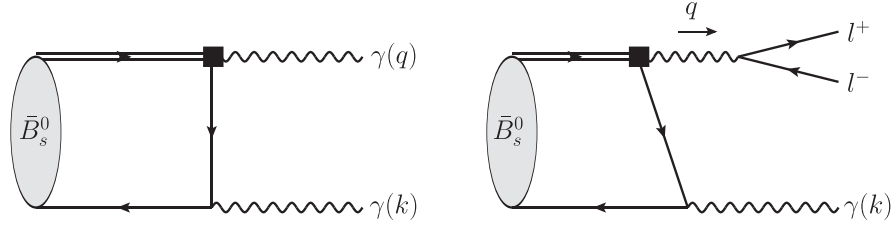


FIG. 1. The leading-order Feynman diagram of  $\bar{B}_s \rightarrow \gamma\gamma$  and  $\bar{B}_s \rightarrow \gamma\ell\bar{\ell}$  decay, where the other two diagrams due to the exchange of two gauge bosons are not presented.

photon from the QED vertex respectively, and we have employed the on shell condition  $l^2 = m_s^2$  in the above equation. In the light cone coordinate system, a momentum  $a^\mu$  can be written as  $a = (n_- \cdot a/2, n_+ \cdot a/2, a_\perp)$ . According to our power counting rule, the soft momentum scales as  $l \sim m_b(\lambda, \lambda, \lambda)$ , and collinear momentum scales as  $k \sim m_b(\lambda^2, 1, \lambda)$ . As a result, the leading-power term which is given in the first line of Eq. (11) scales as  $1/(\lambda m_b)$ . We assume the strange quark mass  $m_s \sim \lambda m_b$ , then the second term in the second line of Eq. (11) is at subleading power, similar to the first term which has been extensively studied in [4]. A straightforward calculation of the second term at tree level leads to the following expression

$$T_{7,\alpha\beta}^{m_s, \text{NLP}} = -[iQ_s \bar{m}_b(\nu) m_s f_{B_s} m_{B_s}] [g_{\alpha\beta}^\perp - i\epsilon_{\alpha\beta}^\perp] \times \int_0^\infty d\omega \frac{\phi_B^-(\omega, \mu)}{\omega}, \quad (12)$$

where the endpoint singularity appear, since the LCDA  $\phi_B^-(\omega, \mu)$  does not vanish when  $\omega \rightarrow 0$ . In the following we evaluate the mass term contribution to the  $\bar{B}_s \rightarrow \gamma\gamma$  and  $\bar{B}_s \rightarrow \gamma\ell\bar{\ell}$  decays with the dispersion approach.

### A. The contribution from the quark mass term in $\bar{B}_s \rightarrow \gamma\gamma$

We start from the correlation function

$$\tilde{T}_7^{\mu\nu}(k, q) = 2\bar{m}_b(\nu) \int d^4x e^{ik \cdot x} \langle 0 | T \{ j_s^\nu(x), [\bar{s} \sigma^{\alpha\mu} q_\alpha P_R b](0) \} | \bar{B}_s(k+q) \rangle |_{k^2 < 0} + [k \leftrightarrow q, \nu \leftrightarrow \mu], \quad (13)$$

where  $k$  is the momentum of the interpolation electromagnetic current  $j_s^\mu = Q_s [\bar{s} \gamma^\mu s]$ . It is regarded to be a hard-collinear mode, i.e.,  $|k^2| \sim m_b \Lambda$  and  $k^2 < 0$ , so that the correlation function can be calculated using a perturbation approach. This correlation function is induced by the electromagnetic penguin operator which gives rise to the left-handed amplitude, therefore it takes the following form

$$\begin{aligned} \tilde{T}_7^{\mu\nu} &= i(g_\perp^{\mu\nu} - i\epsilon_\perp^{\mu\nu}) \bar{m}_b Q_s m_{B_s}^2 \tilde{F}_7, \\ \tilde{F}_7 &= \tilde{F}_{7,\text{LP}} + \tilde{F}_{7,\text{NLP}}^{m_s} + \tilde{F}_{7,\text{NLP}}^{\text{other}}, \end{aligned} \quad (14)$$

where the scalar correlation function can be expressed as the factorization form after a calculation on the partonic level

$$\begin{aligned} \tilde{F}_{7,\text{LP}} &= \hat{U}_1(m_b, \mu_h, \mu) \hat{U}_2(m_b, \mu_h, \mu) K^{-1}(m_b, \mu_h) C_{T_1}^{(A0)} f_{B_s} \\ &\times \int_0^\infty \frac{\phi_B^+(\omega)}{\omega - n \cdot k} \tilde{J}(n \cdot k, \omega, \mu) d\omega, \end{aligned} \quad (15)$$

$$\tilde{F}_{7,\text{NLP}}^{m_s} = - \left( f_{B_s} \frac{m_s}{m_{B_s}} \frac{n \cdot q}{n \cdot k} \right) \int_0^\infty \frac{\phi_B^-(\omega)}{\omega - n \cdot k} d\omega. \quad (16)$$

The leading power factorization formula (15) has been derived in [4]. The  $n \cdot k$  in the denominator of formula (16) regularize the endpoint singularity, at the cost of the nonphysical off shellness of the photon. The on shell limit is to be taken after removing the singularity, then the on shell condition will be recovered and the correlation function turns to the physical matrix element.  $\tilde{F}_{7,\text{NLP}}^{\text{other}}$  denotes the power suppressed terms other than the strange quark mass contribution, and it reduces to  $F_{7,L}^{\text{fac,NLP}}$  when the photon momentum is taken to be on shell. The difference between  $\tilde{F}_{7,\text{NLP}}^{\text{other}}$  and  $F_{7,L}^{\text{fac,NLP}}$  is further suppressed by the small parameter  $\lambda$  compared with the resolved photon contribution relative to the leading power contribution, and it will be neglected. The correlation function will be also expressed in terms of hadronic parameters after inserting the complete set of hadronic states and isolate the ground state contribution. The hadronic form factors relevant to the  $B \rightarrow V$  transitions induced by the tensor current are defined as

$$\begin{aligned}
 \langle 0 | \bar{q} \gamma_\mu q | V(k, \epsilon) \rangle &= i a_V^{(q)} f_V m_V \epsilon_\mu(k), \\
 \langle V(k, \epsilon^*) | \bar{q} \sigma_{\mu\nu} q^\nu b | \bar{B}_s(k+q) \rangle &= 2 a_V^{(q)} T_1(q^2) \epsilon_{\mu\rho\sigma} \epsilon^{*\nu}(k) k^\rho q^\sigma, \\
 \langle V(k, \epsilon^*) | \bar{q} i \sigma_{\mu\nu} \gamma_5 q^\nu b | \bar{B}_s(k+q) \rangle &= a_V^{(q)} T_2(q^2) [(m_B^2 - m_V^2) \epsilon_\mu^*(k) - (\epsilon^* \cdot q)(2k+q)_\mu] \\
 &\quad + a_V^{(q)} T_3(q^2) (\epsilon^* \cdot q) \left[ q_\mu - \frac{q^2}{m_B^2 - m_V^2} (2k+q)_\mu \right], \tag{17}
 \end{aligned}$$

where the flavor factor  $a_V^{(q)}$  comes from the quark structure of the vector mesons, and in this work  $a_\phi^{(s)} = 1$  will be employed. The hadronic representation of the correlation functions then reads,

$$\tilde{T}_7^{\mu\nu} = i(g_\perp^{\mu\nu} - i\epsilon_\perp^{\mu\nu}) \bar{m}_b m_{B_s}^2 \left\{ \frac{Q_s f_V m_V}{m_V^2 - k^2} \left[ \frac{n_+ k}{m_{B_s}} T_1(q^2) + T_2(q^2) \right] + \frac{1}{\pi} \int_{\omega_s}^\infty d\omega' \frac{\rho^{\text{had}}(\omega')}{\omega' - n_- k - i0} \right\}. \tag{18}$$

Accordingly, the scalar correlation function  $\tilde{F}_7$  at the hadronic level is written by

$$\tilde{F}_{7,\text{LP}} + \tilde{F}_{7,\text{NLP}}^{m_s} + \tilde{F}_{7,\text{NLP}}^{\text{other}} = \frac{f_V m_V}{m_V^2 - k^2} \left[ \frac{n_+ k}{m_{B_s}} T_1(q^2) + T_2(q^2) \right] + \frac{1}{\pi} \int_{\omega_s}^\infty d\omega' \frac{\rho^{\text{had}}(\omega')}{\omega' - n_- k - i0}. \tag{19}$$

Matching the two different representations of the correlation functions with the parton-hadron duality; namely, equalizing the dispersion integral in the QCD expression and the hadronic expression of the correlation function above the threshold, and performing the Borel transformation with respect to the variable  $n_- k$ , we obtain the sum rules for the form factors relative in QCD,

$$\frac{n_+ k}{m_{B_s}} T_1(q^2) + T_2(q^2) = \frac{n_+ k}{f_V m_V \pi} \int_0^{\omega_s} \exp\left(\frac{m_V^2 - n_+ k \omega'}{n_+ k \omega_M}\right) (\text{Im}_{\omega'} \tilde{F}_{7,\text{LP}} + \text{Im}_{\omega'} \tilde{F}_{7,\text{NLP}}^{m_s} + \text{Im}_{\omega'} \tilde{F}_{7,\text{NLP}}^{\text{other}}) d\omega. \tag{20}$$

The procedure of evaluation of the above form factors is actually the  $B$ -meson light cone sum rules [24,25], which has been used to calculate various heavy-to-light transition form factors [26–31]. With the specific expression of the term  $\frac{n_+ k}{m_{B_s}} T_1(q^2) + T_2(q^2)$  in hand, we substitute Eq. (20) into Eq. (19), replace the continuum states contribution by the QCD result above the threshold in (19), and take the limit  $n_- k \rightarrow 0$ , and the scalar correlation function  $\tilde{F}_7$  turns to the physical amplitude  $F_7$ ,

$$\begin{aligned}
 F_7 &= \frac{1}{\pi} \int_0^\infty \frac{\text{Im}_{\omega'} \tilde{F}_{7,\text{LP}}}{\omega'} d\omega' + \frac{1}{\pi} \int_0^\infty \frac{\text{Im}_{\omega'} \tilde{F}_{7,\text{NLP}}^{\text{other}}}{\omega'} d\omega' + \frac{1}{\pi} \int_0^{\omega_s} \left[ \frac{n_+ k}{m_V^2} \exp\left(\frac{m_V^2 - n_+ k \omega'}{n_+ k \omega_M}\right) - \frac{1}{\omega'} \right] \text{Im}_{\omega'} \tilde{F}_{7,\text{LP}} \\
 &\quad + \frac{1}{\pi} \int_0^{\omega_s} \frac{n_+ k}{m_V^2} \exp\left(\frac{m_V^2 - n_+ k \omega'}{n_+ k \omega_M}\right) \text{Im}_{\omega'} \tilde{F}_{7,\text{NLP}}^{m_s} d\omega' + \frac{1}{\pi} \int_{\omega_s}^\infty \frac{\text{Im}_{\omega'} \tilde{F}_{7,\text{NLP}}^{m_s}}{\omega'} d\omega', \tag{21}
 \end{aligned}$$

where the first line corresponds to the leading-power contribution and the factorizable NLP contribution  $F_{7,L}^{\text{fac,NLP}}$  in [4], and the second line is identical to resolved photon contribution. Consequently, we can organize the NLP quark mass corrections to the form factors of  $B_s \rightarrow \gamma\gamma$  as the last line. Inserting the specific expression of the imaginary part of  $\tilde{F}_{7,\text{NLP}}^{m_s}$ , we arrive at the final expression of the strange mass term with the dispersion approach as

$$F_{7,\text{NLP}}^{m_s} = -\frac{Q_s f_{B_s} \bar{m}_b m_s}{m_{B_s}^2} \left\{ \frac{m_{B_s}}{m_\phi^2} \int_0^{\omega_s} \exp\left(\frac{m_\phi^2 - m_{B_s} \omega'}{m_{B_s} \omega_M}\right) \phi_B^-(\omega') d\omega' + \int_{\omega_s}^\infty \frac{\phi_B^-(\omega')}{\omega'} d\omega' \right\}, \tag{22}$$

where we used  $n_+ k = n_- q = m_{B_s}$  and  $m_V \equiv m_\phi$ , and the threshold parameter and Borel parameter

$$\omega_s = \frac{s_0}{n_+ k} \sim \mathcal{O}\left(\frac{\Lambda_{\text{QCD}}^2}{m_{B_s}}\right), \quad \omega_M = \frac{M^2}{n_+ k} \sim \mathcal{O}\left(\frac{\Lambda_{\text{QCD}}^2}{m_{B_s}}\right). \tag{23}$$

Noted here, the well-known hierarchy structure of weak interaction also clearly emerges in quark mass corrections.

### B. The contribution of the quark mass term in $\bar{B}_s \rightarrow \gamma \ell \bar{\ell}$

The subleading power contribution to the  $\bar{B}_s \rightarrow \gamma \ell \bar{\ell}$  decays from the strange quark mass effect as well as the resolved photon contribution is not considered in [23], we formally work out the factorization formula of quark mass contribution first. Following [23], we divide the correlation functions relevant to this process into A-type and B-type, which take the following form respectively

$$\begin{aligned} T_i^{\mu\nu} &= \int d^4x e^{ikx} \langle 0 | T \{ Q_s [\bar{s} \gamma^\nu s](x), [\bar{q} \gamma^\mu P_L b](0) \} | \bar{B}_s \rangle, \quad i = 9, 10 \\ T_{7A}^{\mu\nu} &= \frac{2\bar{m}_b}{q^2} \int d^4x e^{ikx} \langle 0 | T \{ Q_s [\bar{s} \gamma^\nu s](x), [\bar{q} i \sigma^{\mu\alpha} q_\alpha P_R b](0) \} | \bar{B}_s \rangle, \\ T_{7B}^{\mu\nu} &= \frac{2\bar{m}_b}{q^2} \int d^4x e^{iqx} \langle 0 | T \{ Q_s [\bar{s} \gamma^\mu s](x), [\bar{q} i \sigma^{\nu\alpha} k_\alpha P_R b](0) \} | \bar{B}_s \rangle. \end{aligned} \quad (24)$$

After contraction of the strange quark field, it is straightforward to isolate the quark mass term and obtain the related factorization formula directly

$$\begin{aligned} \tilde{T}_{9,10}^{\mu\nu, m_s} &= (g_\perp^{\mu\nu} - i\epsilon_\perp^{\mu\nu}) \frac{Q_s f_{B_s} m_{B_s} m_s}{4 n_+ k} \int_0^\infty \frac{\phi_B^-(\omega)}{\omega} d\omega + (g_\perp^{\mu\nu} + i\epsilon_\perp^{\mu\nu}) \frac{Q_s f_{B_s} m_{B_s} m_s}{4 n_+ k} \int_0^\infty \frac{\phi_B^+(\omega)}{\omega} d\omega, \\ \tilde{T}_{7A}^{\mu\nu, m_s} &= -(g_\perp^{\mu\nu} - i\epsilon_\perp^{\mu\nu}) \frac{2\bar{m}_b}{q^2} \frac{Q_s f_{B_s} m_{B_s} n_- q}{4 n_+ k} \int_0^\infty \frac{\phi_B^-(\omega)}{\omega} d\omega - (g_\perp^{\mu\nu} + i\epsilon_\perp^{\mu\nu}) \frac{2\bar{m}_b}{q^2} \frac{Q_s f_{B_s} m_{B_s} n_+ q}{4 n_+ k} \int_0^\infty \frac{\phi_B^+(\omega)}{\omega} d\omega, \\ \tilde{T}_{7B}^{\mu\nu, m_s} &= -(g_\perp^{\mu\nu} - i\epsilon_\perp^{\mu\nu}) \frac{2\bar{m}_b}{q^2} \frac{Q_s f_{B_s} n_+ k m_s}{4} \int_0^\infty \frac{\phi_B^-(\omega)}{\omega - n_+ q} d\omega. \end{aligned} \quad (25)$$

From the above equations, it is obvious that there is no endpoint singularity in the B-type contribution for the existence of  $n_+ q$  in the denominator, and no endpoint singularity in the right-handed amplitudes since they are proportional to the first inverse moment  $1/\lambda_{B_s}$ . While for the other amplitudes, the endpoint singularity arises due to the endpoint behavior of the LCDAs of the  $B$ -meson. Following the same procedure with  $\bar{B}_s \rightarrow \gamma \gamma$  decay, we start from the correlation function in which the momentum related to the electromagnetic current is taken to be off mass shell, then the endpoint singularity is regularized. For the convolution with the integration variable below the threshold parameter, we express the correlation functions with the help of hadronic form factors

$$\begin{aligned} [T_{7A}^{\mu\nu, \text{LP}} + T_{7A}^{\mu\nu, m_s}]|_{\omega < \omega_s} &= \frac{1}{2} (g_\perp^{\mu\nu} - i\epsilon_\perp^{\mu\nu}) \frac{\bar{m}_b}{q^2} \frac{Q_s f_V m_V m_{B_s}}{m_V^2 - k^2} [n_+ k T_1(q^2) + m_{B_s} T_2(q^2)], \\ [T_{9,10}^{\mu\nu, \text{LP}} + T_{9,10}^{\mu\nu, m_s}]|_{\omega < \omega_s} &= \frac{1}{4} (g_\perp^{\mu\nu} - i\epsilon_\perp^{\mu\nu}) \frac{f_V m_V Q_s}{m_V^2 - k^2} [n_+ k V(q^2) + m_{B_s} A_1(q^2)]. \end{aligned} \quad (26)$$

In the above equation we do not include the other power suppressed contribution since they are irrelevant to the extraction of the quark mass contribution and the resolve photon effect corresponding to the lead power amplitude. The  $B \rightarrow V$  form factors induced by the vector and axial vector current are defined by

$$\begin{aligned} \langle V(k, \epsilon^*) | \bar{q} \gamma_\mu b | \bar{B}(k+q) \rangle &= -\frac{2ia_V^{(q)} V(q^2)}{m_B + m_V} \epsilon_{\mu\nu\rho\sigma} \epsilon^{*\nu} k^\rho q^\sigma, \\ \langle V(k, \epsilon^*) | \bar{q} \gamma_\mu \gamma_5 b | \bar{B}(k+q) \rangle &= \frac{2m_V \epsilon^* \cdot q}{q^2} q_\mu a_V^{(q)} A_0(q^2) + (m_B + m_V) \left[ \epsilon_\mu^* - \frac{\epsilon^* \cdot q}{q^2} q_\mu \right] a_V^{(q)} A_1(q^2) \\ &\quad - \frac{\epsilon^* \cdot q}{m_B + m_V} \left[ (2k+q)_\mu - \frac{m_B^2 - m_V^2}{q^2} q_\mu \right] a_V^{(q)} A_2(q^2). \end{aligned} \quad (27)$$

Similar to Eq. (20) the LCSR of the form factors  $V(q^2)$  and  $A_i(q^2)$  can be obtained using the dispersion integral of the scalar functions which are defined through the Lorentz decomposition of the correlation functions in Eq. (24) as follows:

$$T_i^{\mu\nu}(k, q) = E_\gamma \left[ g_\perp^{\mu\nu} \left( F_L^{(i)} - F_R^{(i)} \right) - i\epsilon_\perp^{\mu\nu} \left( F_L^{(i)} + F_R^{(i)} \right) \right]. \quad (28)$$

Inserting the LCSR of the form factors  $V(q^2)$ ,  $A_i(q^2)$ ,  $T_i(q^2)$  into the correlation function (24), we arrive at the final expressions of the power-suppressed resolved photon contribution  $F_{\text{soft},L}^i$ , the quark mass dependent amplitudes  $F_{m,L}^i$ , and the explicit expression reads

$$\begin{aligned}
 F_{\text{soft},L}^{(9,10)} &= \frac{Q_s f_{B_s} m_{B_s}}{4E_\gamma} \int_0^{\omega_s} \left\{ \frac{2E_\gamma}{m_\phi^2} \exp\left(\frac{m_\phi^2 - 2E_\gamma\omega'}{2E_\gamma\omega_M}\right) - \frac{1}{\omega'} \right\} \phi_B^+(\omega') d\omega', \\
 F_{\text{soft},L}^{(7A)} &= -\frac{2\bar{m}_b Q_s f_{B_s} m_{B_s}^2}{q^2 4E_\gamma} \int_0^{\omega_s} \left\{ \frac{2E_\gamma}{m_\phi^2} \exp\left(\frac{m_\phi^2 - 2E_\gamma\omega'}{2E_\gamma\omega_M}\right) - \frac{1}{\omega'} \right\} \phi_B^+(\omega') d\omega', \\
 F_{m,L}^{(9,10)} &= \frac{Q_s f_{B_s} m_{B_s} m_s}{8E_\gamma^2} \left\{ \int_0^{\omega_s} d\omega' \frac{2E_\gamma}{m_\phi^2} \exp\left(\frac{m_\phi^2 - 2E_\gamma\omega'}{2E_\gamma\omega_M}\right) \phi_B^-(\omega') + \int_{\omega_s}^\infty \frac{\phi_B^-(\omega')}{\omega'} d\omega' \right\}, \\
 F_{m,L}^{(7A)} &= -\frac{2\bar{m}_b Q_s f_{B_s} m_{B_s}^2 m_s}{q^2 8E_\gamma^2} \left\{ \int_0^{\omega_s} d\omega' \frac{2E_\gamma}{m_\phi^2} \exp\left(\frac{m_\phi^2 - 2E_\gamma\omega'}{2E_\gamma\omega_M}\right) \phi_B^-(\omega') + \int_{\omega_s}^\infty \frac{\phi_B^-(\omega')}{\omega'} d\omega' \right\}. \quad (29)
 \end{aligned}$$

The other amplitudes are factorizable, and we present the factorization formula as follows:

$$\begin{aligned}
 F_{m,L}^{(7B)} &= -\frac{2\bar{m}_b Q_s f_{B_s} m_s}{q^2 2} \int_0^\infty \frac{\phi_B^-(\omega)}{\omega - q^2/m_{B_s}} d\omega, \\
 F_{m,R}^{(9,10)} &= \frac{Q_s f_{B_s} m_{B_s} m_s}{8E_\gamma^2} \int_0^\infty \frac{\phi_B^+(\omega)}{\omega} d\omega, \\
 F_{m,R}^{(7A)} &= -\frac{2\bar{m}_b Q_s f_{B_s} m_{B_s} (m_{B_s} - 2E_\gamma) m_s}{q^2 8E_\gamma^2} \int_0^\infty \frac{\phi_B^+(\omega)}{\omega} d\omega, \\
 F_{m,R}^{7B} &= 0, \quad (30)
 \end{aligned}$$

The helicity amplitudes corresponding to the resolved photon contribution and the strange quark effects are then given by

$$\begin{aligned}
 \sum_{i=1}^9 \eta_i C_i F_{\text{soft},h}^{(i)} &= C_7^{\text{eff}} F_{\text{soft},h}^{(7A)} + C_9^{\text{eff}} F_{\text{soft},h}^{(9)} \quad h = L, R, \\
 \sum_{i=1}^9 \eta_i C_i F_{m,h}^{(i)} &= C_7^{\text{eff}} (F_{m,h}^{(7A)} + F_{m,h}^{(7B)}) + C_9^{\text{eff}} F_{m,h}^{(9)} \quad h = L, R. \quad (31)
 \end{aligned}$$

TABLE I. Input parameters in the numerical calculations.

Parameter	Value	Ref.	Parameter	Value	Ref.
$m_{B_s}$	5.36688 GeV	[38]	$m_\phi$	1.01946 GeV	[38]
$f_{B_s} _{N_f=2+1+1}$	230.3 MeV	[39]	$\bar{m}_b(4.8 \text{ GeV})$	4.101 GeV	[38]
$\bar{m}_s(2 \text{ GeV})$	$92.9 \pm 0.7 \text{ MeV}$	[38]	$\lambda_{B_s}$	$0.40 \pm 0.15 \text{ GeV}$	[23]
$\alpha_s^{(5)}(m_Z)$	$0.1188 \pm 0.0017$	[38]	$\tau_{B_s}$	$(1.527 \pm 0.011) \text{ ps}$	[38]
$\{\hat{\sigma}_{B_s}^{(1)}(\mu_0), \hat{\sigma}_{B_s}^{(2)}(\mu_0)\}$	$\{0.0 \pm 0.7, 0.0 \pm 6.0\}$	[23]	$\{M_\phi^2, s_\phi^0\}$	$\{1.9 \pm 0.5, 1.6 \pm 0.1\} \text{ GeV}^2$	[30]

#### IV. NUMERICAL ANALYSIS

In this section we will evaluate the numerical results of the quark mass contribution to the  $\bar{B}_s \rightarrow \gamma\gamma$  and  $\bar{B}_s \rightarrow \gamma\ell\bar{\ell}$  decays and the resolved photon contribution to  $\bar{B}_s \rightarrow \gamma\ell\bar{\ell}$  decay. We firstly discuss the nonperturbative hadronic inputs entering the factorized expressions of the helicity amplitudes. The leptonic decay constant of the  $B_s$  meson is taken from the average values of Lattice simulation [32]. The two-particle  $B_s$  meson distribution amplitudes in HQET serve as the fundamental ingredients in the factorization formulas and the expression of the amplitudes from the dispersion approach. Following [14] we will introduce the general three-parameter ansatz for the leading-twist LCDA  $\phi_B^+(\omega, \mu_0)$

$$\begin{aligned}
 \phi_B^+(\omega, \mu_0) &= \int_0^\infty ds \sqrt{ws} J_1(2\sqrt{ws}) \eta_+(s, \mu_0), \\
 \eta_+(s, \mu_0) &= {}_1F_1(\alpha; \beta; -s\omega_0), \quad (32)
 \end{aligned}$$

where  $J_1(x)$  is the Bessel function, and  ${}_1F_1(\alpha, \beta; x)$  is a hypergeometric function. It is useful to define the first inverse moment and the inverse-logarithmic moments of the leading-twist  $B_s$ -meson LCDA

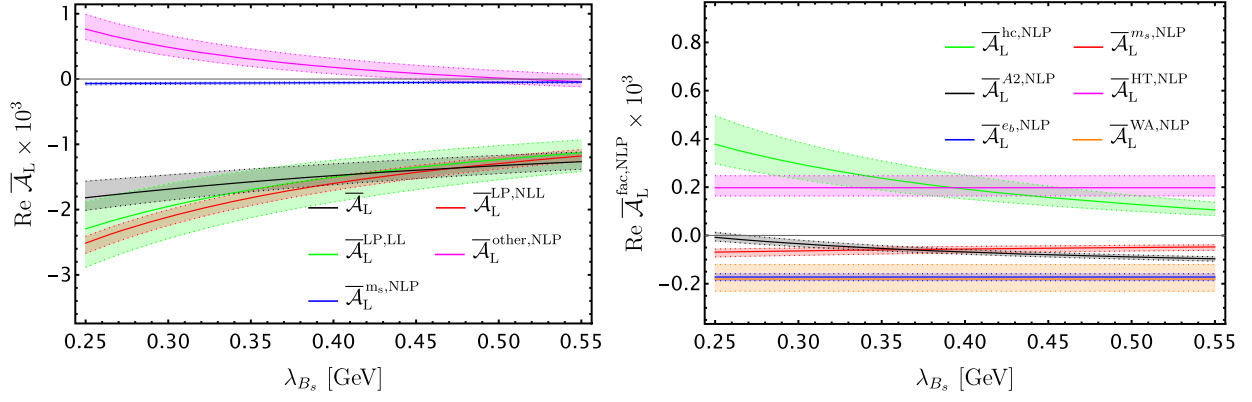


FIG. 2. The leading power and various NLP amplitudes in  $\bar{B}_s \rightarrow \gamma\gamma$  decays as a function of  $\lambda_{B_s}$ . Except for the strange quark mass contribution, the other amplitudes are from Ref. [4].

$$\lambda_{B_s}^{-1}(\mu) = \int_0^\infty d\omega \frac{\phi_B^+(\omega, \mu)}{\omega}$$

$$\hat{\sigma}_{B_s}^{(n)}(\mu) = \lambda_{B_s}(\mu) \int_0^\infty \frac{d\omega}{\omega} \left[ \ln\left(\frac{\lambda_{B_s}(\mu)}{\omega}\right) - \gamma_E \right]^n \phi_B^+(\omega, \mu).$$
(33)

The shape parameter  $\lambda_{B_s}$  and the associated inverse-logarithmic moments  $\hat{\sigma}_{B_s}^{(n)}$  are related to the parameters  $\omega_0$ ,  $\alpha$ ,  $\beta$  with the following identities

$$\lambda_{B_s}(\mu_0) = \left( \frac{\alpha - 1}{\beta - 1} \right) \omega_0,$$

$$\hat{\sigma}_{B_s}^{(1)}(\mu_0) = \psi(\beta - 1) - \psi(\alpha - 1) + \ln\left(\frac{\alpha - 1}{\beta - 1}\right),$$

$$\hat{\sigma}_{B_s}^{(2)}(\mu_0) = [\hat{\sigma}_{B_s}^{(1)}(\mu_0)]^2 + \psi^{(1)}(\alpha - 1) - \psi^{(1)}(\beta - 1) + \frac{\pi^2}{6},$$
(34)

so that the parameter  $\alpha$ ,  $\beta$ ,  $\omega_0$  can be determined through  $\lambda_{B_s}$  and  $\hat{\sigma}_{B_s}^{(n)}$ . However, even the inverse moment  $\lambda_{B_s}$  has not been satisfactorily constrained albeit that distinct techniques and strategies has been employed to investigate this parameter since it is defined by a nonlocal operator [13,14,18,26,28,33–37]. Consequently, we will vary the input value of  $\lambda_{B_s}$  in the conservative interval as presented in Table I. For the associated inverse-logarithmic moments  $\hat{\sigma}_{B_s}^{(n)}$ , we adopt the same values as [4]. The two-particle twist-3 LCDAs of  $B_s$ -meson are also of great importance in our calculation, we adopt the following model

$$\phi_{B_s}^{-\text{WW}}(\omega, \mu_0) = \int_\omega^\infty d\rho f(\rho)$$
(35)

$$\phi_{B_s}^{-\text{tw}3}(\omega, \mu_0) = \frac{1}{6} \kappa(\mu_0) [\lambda_E^2(\mu_0) - \lambda_H^2(\mu_0)]$$

$$\times \left[ \omega^2 f'(\omega) + 4\omega f(\omega) - 2 \int_\omega^\infty d\rho f(\rho) \right]$$
(36)

with

$$\int_0^\infty d\omega f(\omega) = \lambda_{B_s}^{-1}(\mu_0),$$

$$\int_0^\infty d\omega \omega f(\omega) = 1,$$

$$\int_0^\infty d\omega \omega^2 f(\omega) = \frac{4}{3} \bar{\Lambda},$$

$$\kappa^{-1}(\mu_0) = \frac{1}{2} \int_0^\infty d\omega \omega^3 f(\omega)$$

$$= \bar{\Lambda}^2 + \frac{1}{6} [2\lambda_E^2(\mu_0) + \lambda_H^2(\mu_0)].$$
(37)

For the other parameters such as the running quark mass, the threshold parameter, and the Borel mass, we also follow the same choice as [4]. The specific vales are given in Table I.

Inputting all the values of the parameters into the analytic formulas, we can obtain the numerical results for various decay amplitudes and the phenomenological observables.

TABLE II.  $CP$ -averaged branching ratio of  $B_s \rightarrow \gamma\gamma$  decays with uncertainty in unit of  $10^{-7}$ .

Contributions	Central value	Total error	Error from $\lambda_{B_s}$
Leading power(LP)	3.87	+5.69 -1.85	+5.66 -1.77
LP + NLP	3.25	+2.09 -1.73	+1.54 -0.80
LP + NLP + quark mass	3.49	+2.21 -1.80	+1.67 -0.87



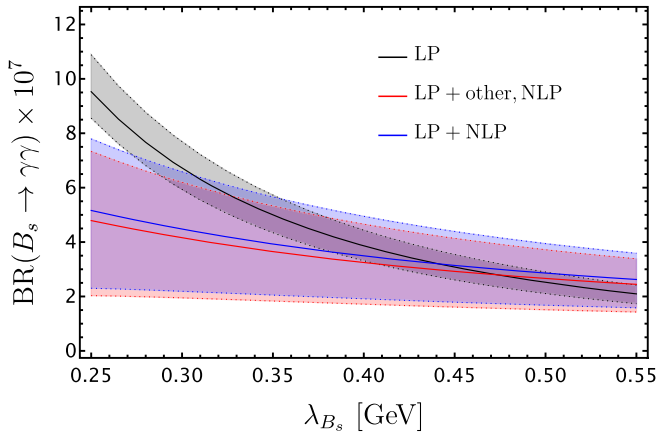


FIG. 3. The branching ratio of  $B_s \rightarrow \gamma\gamma$  decays as a function of  $\lambda_{B_s}$ : (1) With only the leading-power contribution; (2) With NLP contributions except for the strange quark mass term; (3) The complete contribution.

In what follows, we first present the numerical result of the strange quark mass effect in the  $\bar{B}_s \rightarrow \gamma\gamma$  decay. The  $\lambda_{B_s}$  dependence of the real part of the left-handed polarized amplitude from the leading-power contribution, the NLP contribution without quark mass effect, and the full results

are shown in the left panel of Fig. 2. It can be seen that the contribution from the quark mass is a few percent of the full amplitude, which is almost independent of the parameter  $\lambda_{B_s}$ . As a result, it plays a more important rule in the NLP contribution as  $\lambda_{B_s}$  becomes large. The right panel of Fig. 2 exhibits the amplitudes from various sources of NLP contribution, and it is obvious that the cancellation between them highlights the contribution from the quark mass term.

The branching ratio of  $B_s \rightarrow \gamma\gamma$  decay is given in Table II, where the uncertainty is obtained by varying separate input parameters within their ranges and adding the different uncertainties of the form factors in quadrature. The main uncertainty is obviously from the parameter  $\lambda_{B_s}$ . From the central value we can see that the quark mass term can enhance the branching ratio by about 6%, which deserves a reliable study if one intends to precisely determine the parameters in the standard model. In Fig. 3 we plotted the  $\lambda_{B_s}$  dependence of the branching ratio of  $B_s \rightarrow \gamma\gamma$  decay, which can serve as a good method to determine  $\lambda_{B_s}$ . However, the accuracy of the determination of the parameter  $\lambda_{B_s}$  is limited by the large theoretical uncertainty from other parameters. An optional method to improve the accuracy is to perform a global fit together with the other processes.

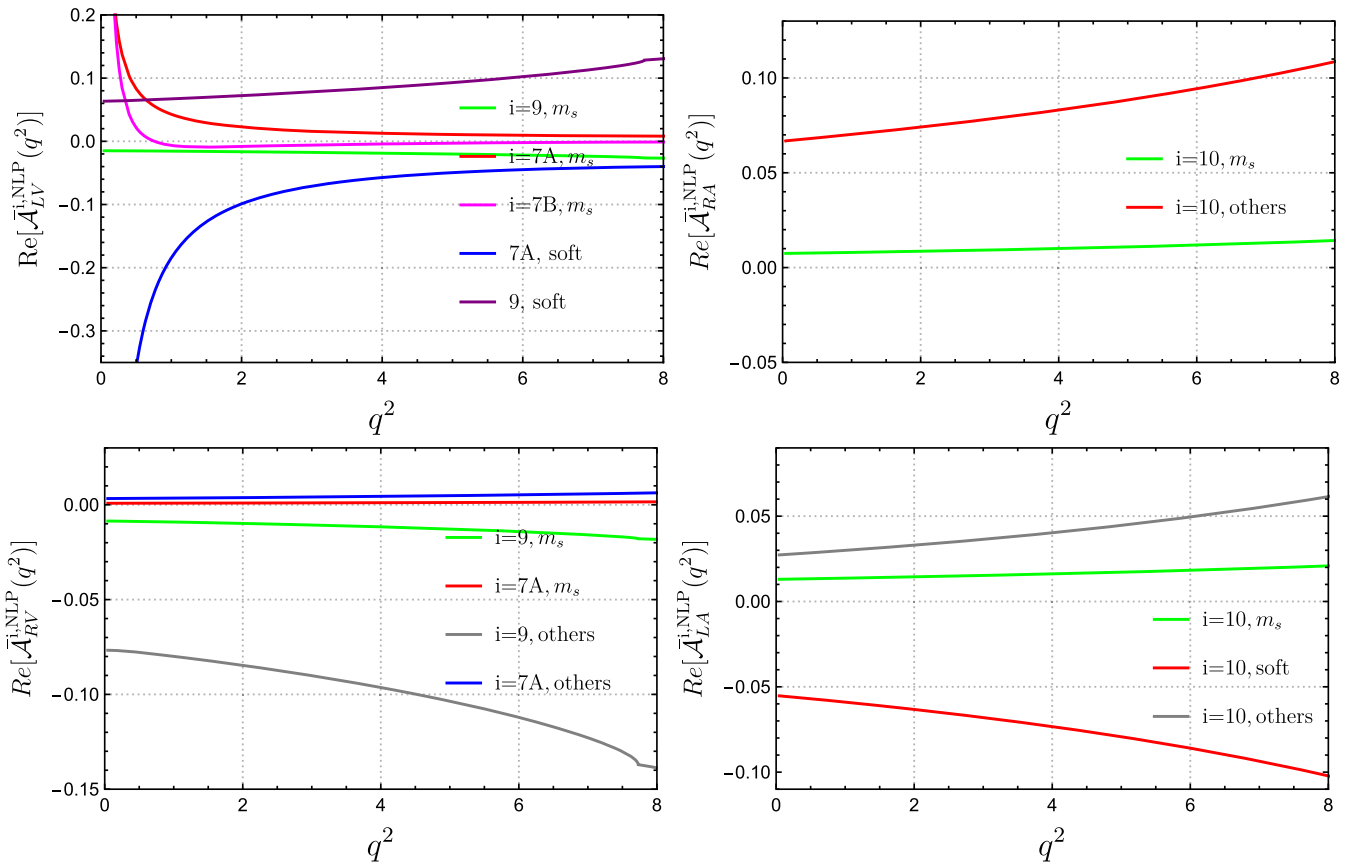


FIG. 4. The quark mass and soft contribution to the real parts of  $\bar{B}_s \rightarrow \gamma\mu^+\mu^-$  decay amplitude  $\bar{A}_{LV,LA}$  [left] and  $\bar{A}_{RV,RA}$  [right] from operator  $P_{9,10}$  and  $P_7$  as a function of  $q^2$ .

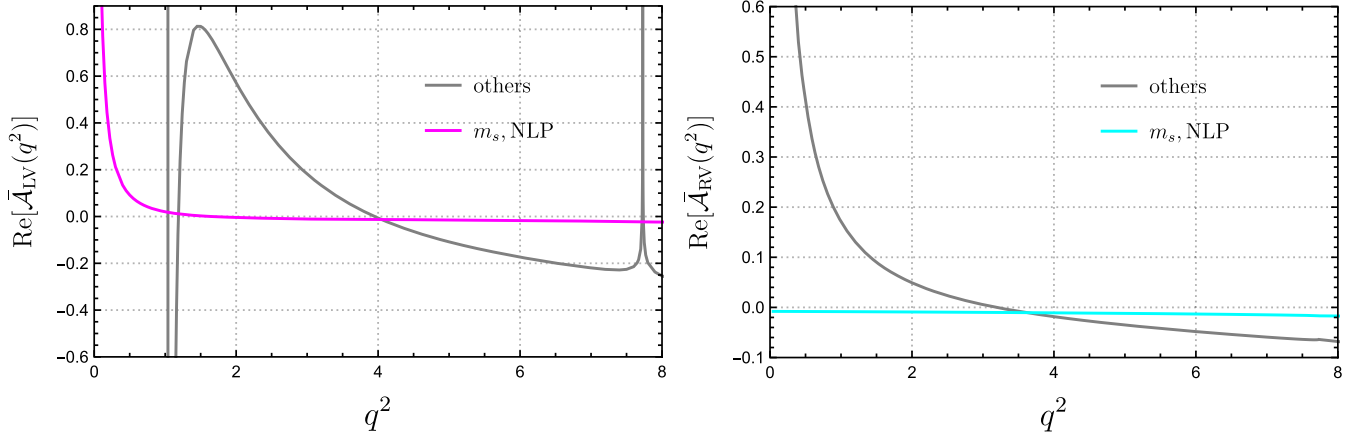


FIG. 5. The quark mass [violet, cyan] contribution to real parts of  $\bar{B}_s \rightarrow \gamma\mu^+\mu^-$  decay amplitude  $\bar{A}_{LA}$  (left) and  $\bar{A}_{RA}$  (right) from operator  $P_7$  and  $P_9$  as a function of  $q^2$ . For comparison, the total results with  $\phi(1020)$  resonance around  $q^2 \simeq 1$  GeV [gray] are also shown.

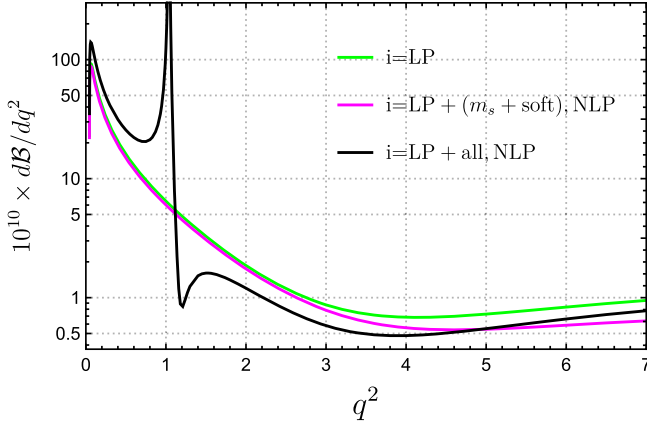


FIG. 6. The  $CP$ -averaged differential branching ratio  $dB/dq^2$  distributions for  $B_s \rightarrow \gamma\mu^+\mu^-$  decay with and without the mass term and soft contribution.

The strange quark mass effect in the  $\bar{B}_s \rightarrow \gamma\mu^+\mu^-$  decay is a bit more complicated since several operators can contribute besides the electromagnetic penguin operator, and the right-handed polarized amplitude can also receive corrections from the strange quark mass effect. The size of the quark mass term induced by the operators  $P_{7,9,10}$  are collected in Fig. 4 as a function of  $q^2$ . We can see that almost all the effects of axial-vector currents or right-helicity amplitudes come from semileptonic operators

TABLE III. Integrated branching ratios (in unit of  $10^{-9}$ ) of  $B_s \rightarrow \gamma\mu^+\mu^-$  decay with and without the quark mass and the soft-photon effect.

Region of $q^2$	$[4m_\mu^2, 6.0]$ GeV <sup>2</sup>	$[4m_\mu^2, 8.64]$ GeV <sup>2</sup>
Without $m_s$ and soft	$12.43^{+3.83}_{-1.93}$	$12.74^{+4.15}_{-2.08}$
With $m_s$ and soft	$12.28^{+3.83}_{-1.93}$	$12.49^{+4.15}_{-2.08}$

$P_{9,10}$ . It is clear that there exists cancellation between different operators, which reduces the total quark mass term contribution. In the amplitude level, the ratio between the quark mass term and the full amplitude is close to that of the  $\bar{B}_s \rightarrow \gamma\gamma$  decays. We exhibit relative magnitude between the quark mass effect and the full amplitude in Fig. 5 induced by  $P_{7,9}$  operators. In this figure, the total results with  $\phi(1020)$  resonance contribution around  $q^2 \simeq 1$  GeV [gray] are also shown. It is obvious that the mass term contribution in the  $\bar{B}_s \rightarrow \gamma\mu^+\mu^-$  decay is negligibly small except for an enhancement from operator  $P_7$  at very small  $q^2$ , which can be seen from Fig. 4.

The differential branching ratio of  $B_s \rightarrow \gamma\mu^+\mu^-$  decay with respect to  $q^2$  is plotted in Fig. 6, where we have included the on shell hadronic state contribution in order to compare with the future data. The quark mass effect is negligible at small  $q^2$  region compared with the large hadronic resonance contribution. The integrated branching ratios are listed in Table III, where we have considered two integration regions  $[4m_\mu^2, 6.0]$  GeV<sup>2</sup> and  $[4m_\mu^2, 8.64]$  GeV<sup>2</sup> of invariant mass of the lepton pair. The uncertainty from the strange quark mass term is also negligible compared with the other error from [23]. The results in this table indicate that the quark mass effect is less important in  $B_s \rightarrow \gamma\mu^+\mu^-$  decay than that in the  $B_s \rightarrow \gamma\gamma$  decay. This is mainly due to the inclusion of the hadronic state contribution at small  $q^2$ , which significantly enhance the total branching ratio.

## V. SUMMARY

The power-suppressed contributions play an important role in the radiative decays  $B_{d,s} \rightarrow \gamma\gamma$  and radiative leptonic decays  $B_{d,s} \rightarrow \gamma\ell\bar{\ell}$ . Some of them are factorizable and can be investigated using a factorization approach; however, the emergence of the endpoint singularity prevents us from

applying the factorization methods to many other contributions. Therefore, one must find some special techniques to deal with the nonfactorizable contributions. The contribution from the quark mass term in the  $B_s \rightarrow \gamma\gamma$  as well as  $B_s \rightarrow \gamma\ell\bar{\ell}$  decays suffers from the endpoint singularities. In the previous study it was parametrized in a model dependent way. In order to reduce the model dependence and improve the theoretical precision, we revisit this NLP contribution with a QCD-inspired approach; namely, the dispersion approach. In this approach, we introduce the  $B_s \rightarrow V$  form factors instead of the arbitrary momentum cutoff to deal with the endpoint singularity; therefore, the prediction power is highly improved. Taking advantage of the dispersion approach, the analytic expression of the quark mass contribution and the resolved photon contribution in the  $B_s \rightarrow \gamma\gamma$  and  $B_s \rightarrow \gamma\ell\bar{\ell}$  decays can be obtained simultaneously.

The numerical results of the NLP contribution to the  $B_s \rightarrow \gamma\gamma$  and  $B_s \rightarrow \gamma\ell\bar{\ell}$  decays from the strange quark mass effect have also been presented. In the  $B_s \rightarrow \gamma\gamma$  decay, the strange quark mass term can give rise to about 6% contribution relative to the total amplitude, which makes

sense if this process is employed to determine the parameters in the standard model. The strange quark mass contribution to the  $B_s \rightarrow \gamma\ell\bar{\ell}$  decays is relatively small, due to the cancellation between the contributions from different operators and the enhancement of large hadronic resonance contribution. The uncertainty of the input parameters is sizable, which renders us from a more accurate prediction so far. However, it is promising to achieve more precise predictions with our improved theoretical method once future experiments can precisely constrain the hadronic parameters.

## ACKNOWLEDGMENTS

We thank Yan-Bing Wei and Hao-Yi Ci for some useful contributions. This work was supported in part by the National Natural Science Foundation of China under Grants No. 12175218 and No. 12070131001 and the National Key Research and Development Program of China under Contract No. 2020YFA0406400. Y. L. S. also acknowledges the Natural Science Foundation of Shandong province with Grant No. ZR2020MA093.

- 
- [1] D. Guadagnoli, M. Reboud, and R. Zwicky, *J. High Energy Phys.* **11** (2017) 184.
  - [2] J. Albrecht, E. Stamou, R. Ziegler, and R. Zwicky, *J. High Energy Phys.* **09** (2020) 139.
  - [3] E. Kou *et al.* (Belle-II Collaboration), *Prog. Theor. Exp. Phys.* **2019**, 123C01 (2019); **2020**, 029201(E) (2020).
  - [4] Y. L. Shen, Y. M. Wang, and Y. B. Wei, *J. High Energy Phys.* **12** (2020) 169.
  - [5] S. W. Bosch and G. Buchalla, *J. High Energy Phys.* **08** (2002) 054.
  - [6] K. G. Chetyrkin, M. Misiak, and M. Munz, *Phys. Lett. B* **400**, 206 (1997); **425**, 414(E) (1998).
  - [7] Z. L. Liu and M. Neubert, *J. High Energy Phys.* **06** (2020) 060.
  - [8] C. W. Bauer, S. Fleming, D. Pirjol, and I. W. Stewart, *Phys. Rev. D* **63**, 114020 (2001).
  - [9] M. Beneke, A. P. Chapovsky, M. Diehl, and T. Feldmann, *Nucl. Phys.* **B643**, 431 (2002).
  - [10] A. Khodjamirian, *Eur. Phys. J. C* **6**, 477 (1999).
  - [11] S. S. Agaev, V. M. Braun, N. Offen, and F. A. Porkert, *Phys. Rev. D* **83**, 054020 (2011).
  - [12] V. M. Braun and A. Khodjamirian, *Phys. Lett. B* **718**, 1014 (2013).
  - [13] Y. M. Wang, *J. High Energy Phys.* **09** (2016) 159.
  - [14] M. Beneke, V. M. Braun, Y. Ji, and Y. B. Wei, *J. High Energy Phys.* **07** (2018) 154.
  - [15] Y. L. Shen, Y. B. Wei, X. C. Zhao, and S. H. Zhou, *Chin. Phys. C* **44**, 123106 (2020).
  - [16] P. Ball, V. M. Braun, and N. Kivel, *Nucl. Phys.* **B649**, 263 (2003).
  - [17] Y. M. Wang and Y. L. Shen, *J. High Energy Phys.* **12** (2017) 037.
  - [18] Y. M. Wang and Y. L. Shen, *J. High Energy Phys.* **05** (2018) 184.
  - [19] Y. L. Shen, Z. T. Zou, and Y. B. Wei, *Phys. Rev. D* **99**, 016004 (2019).
  - [20] Y. L. Shen, Z. T. Zou, and Y. Li, *Phys. Rev. D* **100**, 016022 (2019).
  - [21] Y. L. Shen, J. Gao, C. D. Lü, and Y. Miao, *Phys. Rev. D* **99**, 096013 (2019).
  - [22] T. Janowski, B. Pullin, and R. Zwicky, *J. High Energy Phys.* **12** (2021) 008.
  - [23] M. Beneke, C. Bobeth, and Y. M. Wang, *J. High Energy Phys.* **12** (2020) 148.
  - [24] A. Khodjamirian, T. Mannel, and N. Offen, *Phys. Lett. B* **620**, 52 (2005).
  - [25] F. De Fazio, T. Feldmann, and T. Hurth, *Nucl. Phys.* **B733**, 1 (2006); **B800**, 405(E) (2008).
  - [26] Y.-M. Wang and Y.-L. Shen, *Nucl. Phys.* **B898**, 563 (2015).
  - [27] Y.-L. Shen, Y.-B. Wei, and C.-D. Lü, *Phys. Rev. D* **97**, 054004 (2018).
  - [28] Y.-M. Wang, Y.-B. Wei, Y.-L. Shen, and C.-D. Lü, *J. High Energy Phys.* **06** (2017) 062.
  - [29] C.-D. Lü, Y.-L. Shen, Y.-M. Wang, and Y.-B. Wei, *J. High Energy Phys.* **01** (2019) 024.
  - [30] J. Gao, C. D. Lü, Y. L. Shen, Y. M. Wang, and Y. B. Wei, *Phys. Rev. D* **101**, 074035 (2020).

- [31] Y.-M. Wang and Y.-L. Shen, *J. High Energy Phys.* **02** (2016) 179.
- [32] A. Bazavov *et al.*, *Phys. Rev. D* **98**, 074512 (2018).
- [33] V.M. Braun, D.Y. Ivanov, and G.P. Korchemsky, *Phys. Rev. D* **69**, 034014 (2004).
- [34] H. n. Li, Y.L. Shen, and Y.M. Wang, *Phys. Rev. D* **85**, 074004 (2012).
- [35] H. N. Li, Y.L. Shen, and Y.M. Wang, *J. High Energy Phys.* **02** (2013) 008.
- [36] M. Beneke and J. Rohrwild, *Eur. Phys. J. C* **71**, 1818 (2011).
- [37] A. Khodjamirian, R. Mandal, and T. Mannel, *J. High Energy Phys.* **10** (2020) 043.
- [38] P. A. Zyla *et al.* (Particle Data Group), *Prog. Theor. Exp. Phys.* **2020**, 083C01 (2020).
- [39] S. Aoki *et al.* (Flavour Lattice Averaging Group), *Eur. Phys. J. C* **80**, 113 (2020).